1-1-2014

Equalizer tap length requirement for mode group delay-compensated fiber link with weakly random mode coupling

Neng Bai
University of Central Florida

Guifang Li
University of Central Florida

Equalizer tap length requirement for mode group delay-compensated fiber link with weakly random mode coupling

Neng Bai[1,2,*] and Guifang Li[1,3,4]

[1]*CREOL, The College of Optics & Photonics, University of Central Florida 4000 Central Florida Blvd. Orlando FL, 32816-2700, USA*
[2]*Infinera Corp., 169 West Java Dr. Sunnyvale CA, 94089, USA*
[3]*College of Precision Instrument and Opto-Electronic Engineering, Tianjin University, Tianjin, China*
[4]*li@creol.ucf.edu*
[*]*bneng@creol.ucf.edu*

Abstract: The equalizer tap length requirement is investigated analytically and numerically for differential modal group delay (DMGD) compensated fiber link with weakly random mode coupling. Each span of the DMGD compensated link comprises multiple pairs of fibers which have opposite signs of DMGD. The result reveals that under weak random mode coupling, the required tap length of the equalizer is proportional to modal group delay of a single DMGD compensated pair, instead of the total modal group delay (MGD) of the entire link. By using small DMGD compensation step sizes, the required tap length (RTL) can be potentially reduced by 2 orders of magnitude.

OCIS codes: (060.4230) Multiplexing; (060.2330) Fiber optics communications; (060.2360) Fiber optics links and subsystems.

References and links

1. N. Bai and G. Li, "Adaptive frequency-domain equalization for mode-division multiplexed transmission," Photonics Technology Letters **24**(21), 1918–1921 (2012).
2. K. Ho and J. M. Kahn, "Statistics of group delays in multimode fiber with strong mode coupling," J. Lightwave Technol. **29**(21), 3119–3128 (2011).
3. F. Ferreira, D. Fonseca, A. Lobato, B. Inan, and H. Silva, "Reach improvement of mode division multiplexed systems using fiber splices," Photonics Technology Letters **25**(12), 1091–1094 (2013).
4. M. Li, B. Hoover, S. Li, S. Bickham, S. Ten, E. Ip, Y. Huang, E. Mateo, Y. Shao, and T. Wang, "Low delay and large effective area few-mode fibers for mode-division multiplexing," In *Opto-Electronics and Communications Conference (OECC),* 495–496 (2012).
5. T. Mori, T. Sakamoto, M. Wada, T. Yamamoto, and F. Yamamoto, "Low DMD Four LP Mode Transmission Fiber for Wide-band WDM-MIMO System," in *Optical Fiber Communication Conference/National Fiber Optic Engineers Conference*, (Optical Society of America, 2013), paper OTh3K.1.
6. T. Sakamoto, T. Mori, T. Yamamoto, and S. Tomita, "Differential Mode Delay Managed Transmission Line for WDM-MIMO System Using Multi-Step Index Fiber," J. Lightwave Technol. 30(17), 2783–2787 (2013).
7. S. Randel, R. Ryf, A. Gnauck, M. Mestre, C. Schmidt, R. Essiambre, P. Winzer, R. Delbue, P. Pupalaikis, A. Sureka, Y. Sun, X. Jiang, and R. Lingle, "Mode-multiplexed 6×20-GBd QPSK transmission over 1200-km DGD-compensated few-mode fiber," in Optical Fiber Communication Conference, OSA Technical Digest (Optical Society of America, 2012), paper PDP5C.5.
8. C. Antonelli, A. Mecozzi, M. Shtaif, and P. J. Winzer, "Random coupling between groups of degenerate fiber modes in mode multiplexed transmission," Opt. Express **21**(8), 9484–9490 (2013).
9. F. Yaman, E. Mateo, and T. Wang, "Impact of Modal Crosstalk and Multi-Path Interference on Few-Mode Fiber Transmission," in *Optical Fiber Communication Conference*, OSA Technical Digest (Optical Society of America, 2012), paper OTu1D.2.
10. F. Ferreira, D. Fonseca, and H. Silva, "Design of few-mode fibers with arbitrary and flattened differential mode delay," Photonics Technology Letters **25**(5), 438–441 (2013).
11. L. Grüner-Nielsen, Y. Sun, J. W. Nicholson, D. Jakobsen, K. G. Jespersen, R. Lingle, Jr., and B. Pálsdóttir, "Few mode transmission fiber with low DGD, low mode coupling, and low loss," J. Lightwave Technol. **30**(23), 3693–3698 (2012).

#201102 - $15.00 USD Received 12 Nov 2013; revised 31 Dec 2013; accepted 27 Jan 2014; published 18 Feb 2014

1. Introduction

Mode-division multiplexed transmission using few-mode fiber (FMF) has been considered as a promising candidate to overcome the fundamental capacity limit of the single-mode fiber. However, due to mode coupling and differential mode group delay (DMGD), complicated multiple-input- multiple-output (MIMO) equalizer is required in the coherent receiver to cancel multimode interference. To reduce the complexity of MIMO equalizer, four main approaches have been proposed. The first approach uses computational efficient algorithms, such as frequency-domain equalization (FDE) to save the number of multiplications per symbol [1]. By using FDE, the algorithmic complexity of the equalizer scales logarithmically with the mode group delay (MGD) instead of linearly using time-domain equalization. However, for fiber link whose total MGD is large, FDE still requires long memory length therefore high hardware complexity of FDE. The second approach is to design and fabricate a fiber with ultra-low DMGD. Although, a low DMGD fiber with two LP modes has been reported, for FMF supporting 4 LP modes or more, ultra-low DMGD is difficult to be achieved so far. The third approach is to introduce strong coupling to reduce the channel impulse response spread (CIRS), or the equalizer tap length [2]. Due to the effective index difference between different modes, FMFs are naturally weakly coupled. To intentionally enhance mode coupling, artificial perturbations have to be applied on the fiber. Off-center splicing was proposed in [3] to induce mode coupling. However, the off-center splicing introduces mode-dependent loss which degrades the system performance. The fourth approach is using DMGD-compensated fiber [4–7]. In a DMGD-compensated fiber link, two types of fibers are spliced together. They are: P-type whose DMGD is positive and N-type whose DMGD is negative. By center splicing multiple pairs of these two fibers, the aggregate MGD can be achieved to be very low. So far, DMGD-compensated fiber which can guide 4 LP modes has been demonstrated [5]. If random mode coupling can be neglected, the CIRS of a fully DMGD compensated link virtually vanishes. To minimize random mode coupling, it is possible to design a FMF with large effective refractive index difference. However, with mode coupling, the CIRS could be much larger as was shown in a reported experiment [7]. In this paper, the CIRS and required equalizer tap length for DMGD-compensated links with weak mode coupling is investigated analytically and numerically. Our result shows that by decreasing the DMGD compensation step size, the CIRS of a DMGD-compensated link can be significantly reduced even under moderate mode coupling.

The remainder of the paper is organized as follows. Section 2 describes an analytical model of DMGD-compensated link under the weak mode-coupling assumption. Section 3 presents simulation results of a long-distance DMGD-compensated link and compares the required equalizer tap lengths between analytical and numerical results. Section 4 provides a conclusion.

2. Theory

For a FMF which can guide N LP modes, different modes propagate with different group velocities resulting in different group delays τ_i. The DMGD for the i^{th} mode can be defined as the difference between τ_i and the average MGD of all the modes.

$$\Delta\tau_i = \tau_i - \frac{1}{N}\sum_{j=1}^{N}\tau_j. \tag{1}$$

A DMGDC link comprises 2 types of FMF: P-type and N-type. The DMGD of LP_{01} is positive for P-type fiber while negative for N-type fiber. In a single span of a DMGDC link, two types of FMFs are spliced alternatively as shown in Fig. 1. The adjacent two FMF sections form a DMGD-compensation pair which is the building block of the DMGDC span.

#201102 - $15.00 USD Received 12 Nov 2013; revised 31 Dec 2013; accepted 27 Jan 2014; published 18 Feb 2014

In the zero residual DMGD case, the accumulate DMGDs for every mode group of these two sections satisfy the following Eq.

$$\Delta\tau_i^{(P)} L_P = -\Delta\tau_i^{(N)} L_N \tag{2}$$

where $\Delta\tau_i^{(P)}$ and $\Delta\tau_i^{(N)}$ are the DMGD of the i[th] mode of the P-type and N-type FMF, respectively; L_P and L_N are the lengths of P-type and N-type fiber. If $\Delta\tau_i^{(P)} = -\Delta\tau_i^{(N)}$, L_P equals to L_N which can be defined as compensation step-size. Although DMGD compensation for 4 mode groups has been demonstrated, it may be hard to fully compensated DMGD for all the modes in many-mode fibers in practice. As an approximation, analytical derivation and numerical analyses in this paper consider only zero residual DMGD link. In addition, the delay spread due to degenerate modes is assumed to be neglected small compared to CIRS. Thus we only investigated delay spread between non-degenerate mode groups.

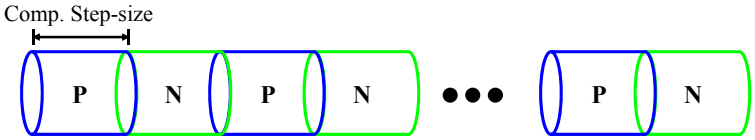

Fig. 1. A single span of DMGDC link.

2.1 Impulse response of a DMGD uncompensated link

A FMF link which has D spatial degrees of freedom can be characterized using a $D \times D$ matrix $\overline{\overline{H}}$. Each element of the matrix (h_{ij}) is an impulse response which lasts a certain period of time. The input-output relationship can be expressed as

$$y_j = \sum_{i=1}^{D} h_{ij} * x_i \tag{3}$$

where x_i and y_j are input signal in the i^{th} mode and output signal in the j^{th} mode. The CIRS equals to the longest length of h_{ij} .In the P type fiber, the slowest mode is named the S mode and the fastest mode is named the F mode. Due to opposite signs of DMGD, S mode in the N type fiber is actually the fastest mode and the F mode is the slowest one. For the case of weakly coupled FMFs, the CIRS corresponds to delay spread ΔT of the FMF:

$$\Delta T = \left(\Delta\tau_s - \Delta\tau_f\right) L \tag{4}$$

where $\Delta\tau_s$ is the MGD of the S mode, $\Delta\tau_f$ is the MGD of the F mode and L is the fiber length of the link. The DMGD is denoted by $\Delta\tau = \Delta\tau_s - \Delta\tau_f$. Since group delay difference between the S and F modes determines the MGD of the link, these two modes are the most critical pair that determines CIRS. The impulse response h_{sf} describes the linear coupling from the S to the F mode along the link, which includes direct coupling between them and indirect coupling via other modes. Due to the weak coupling assumption, indirect coupling is negligible compared to direct coupling. Another consequence of weak coupling is that all modes can be considered as un-depleted and mode coupling can be described by first order perturbation analysis as in [8].Therefore, the link can be simplified as a two-mode system which is illustrated in Fig. 2.

#201102 - $15.00 USD Received 12 Nov 2013; revised 31 Dec 2013; accepted 27 Jan 2014; published 18 Feb 2014

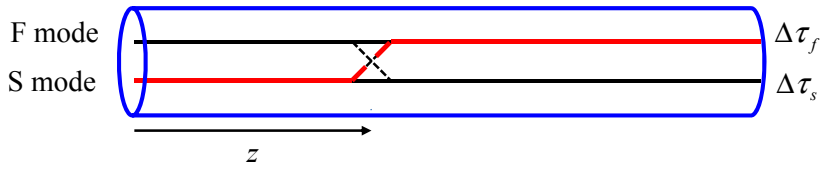

Fig. 2. A single span of DMGD uncompensated fiber.

The two straight lines symbolize the F and the S modes. At location z, signal in the S mode is coupled to that in the F mode with a coupling coefficient $\kappa_{sf}(z)$ where $z \in [0, L]$. The statistics of $\kappa_{sf}(z)$ is assumed to obey normal distribution with zero mean [8] and variance of σ_κ^2 which equals to mode scattering coefficient (MSC) defined in [9]. The path delay ($T_p(z)$) of the coupling light via coupling location z can be calculated

$$T_p(z) = \Delta\tau z + \Delta\tau_f L \tag{5}$$

The impulse response function h_{sf} therefore can be obtained by integrating over all possible coupling paths from beginning to end as

$$\begin{aligned} h_{sf}(t) &= \int_0^L \delta\left(t - \Delta\tau z - \Delta\tau_f L\right)\kappa_{sf}(z)\exp\left(j\Delta\beta_{sf} z + j\beta_f L\right)dz \\ &= \frac{1}{\Delta\tau}\kappa_{sf}\left(\frac{t-\Delta\tau_f L}{\Delta\tau}\right)\exp\left(j\frac{\Delta\beta_{sf}}{\Delta\tau}t - j\frac{\Delta\tau_f\beta_s - \Delta\tau_s\beta_f}{\Delta\tau}L\right) \end{aligned} \tag{6}$$

where β_s and β_f are the propagation constants of the two modes, respectively; $\Delta\beta_{sf}$ is the difference between them. Because $\kappa(z)$ is nonzero for $0 \le z \le L$, the range of t can be calculated as $\Delta\tau_f L \le t \le \Delta\tau_s L$. Inside the integral, the expression describes a decomposed impulse response induced by a single coupling event at location z with coupling strength $\kappa_{sf}(z)$. The exponential term denotes an accumulated phase of the selected path. Since the equalizer needs to cover the non-zero range of the impulse response, the required tap length (RTL) of DMGD uncompensated link, assuming oversampling rate of 2, can be expressed as following

$$N_{taps} = 2\Delta\tau L R_s \tag{7}$$

where R_s is the symbol rate.

2.2 Impulse Response of a DMGD compensated pair

Figure 3(a)-3(b) shows a fiber span with one DMGD compensation pair.

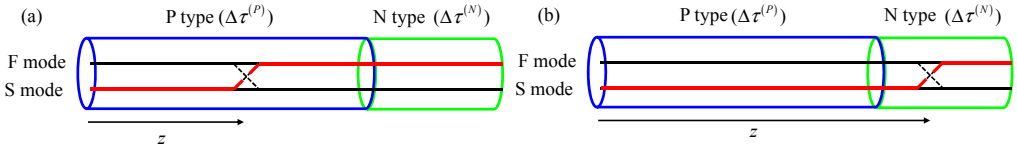

Fig. 3. A single span with one DMGD compensation pair with mode coupling in (a) P type section (Case I), (b) N type section (Case II).

Two cases are discussed in this section: I) mode coupling occurs in the P section; II) mode coupling occurs in the N section. The impulse response for the entire link is thus given by:

#201102 - $15.00 USD Received 12 Nov 2013; revised 31 Dec 2013; accepted 27 Jan 2014; published 18 Feb 2014

$$h_{sf}(t) = h_{sf}^{(I)}(t) + h_{sf}^{(II)}(t) \tag{8}$$

where $h_{sf}^{(I)}(t)$ and $h_{sf}^{(II)}(t)$ are the impulse responses for case I and case II, respectively (not the impulse responses of the respective sections). Following the similar procedure as the derivation of Eq. (6), $h_{sf}^{(I)}(t)$ and $h_{sf}^{(II)}(t)$ can be expressed as the following integrals:

$$h_{sf}^{(I)}(t) = \int_0^{L_P} \delta\left(t - \Delta\tau^{(P)} z\right) \kappa_{sf}^{(P)}(z) \exp\left(j\Delta\beta_{sf}^{(P)} z + j\left(\beta_f^{(P)} L_p + \beta_s^{(N)} L_N\right)\right) dz \tag{9}$$

$$\begin{aligned} h_{sf}^{(II)}(t) = & \int_{L_P}^{L_P+L_N} \delta\left(t - \Delta\tau^{(N)}\left(z - L_N - L_P\right)\right) \kappa_{sf}^{(N)}(z) \\ & \exp\left[j\Delta\beta_{sf}^{(N)} z + j\left(\left(\beta_s^{(P)} - \Delta\beta_{sf}^{(N)}\right) L_p + \beta_f^{(N)} L_N\right)\right] dz \end{aligned} \tag{10}$$

where $\Delta\tau^{(\bullet)}$ is overall DMGD for the P-type or the N-type FMF, $\beta_s^{(\bullet)}$ and $\beta_f^{(\bullet)}$ are propagation constants for slowest and fastest mode in the P-type or the N-type FMF respectively, $\Delta\beta_{sf}^{(\bullet)}$ is the difference between $\beta_s^{(\bullet)}$ and $\beta_f^{(\bullet)}$. Substituting Eqs. (9-10) into Eq. (8), we obtain h_{sf} as:

$$\begin{aligned} h_{sf}(t) = & \frac{1}{\Delta\tau^{(P)}} \kappa_{sf}^{(P)}\left(\frac{t}{\Delta\tau^{(P)}}\right) \exp\left(j\Delta\beta_{sf}^{(P)} \frac{t}{\Delta\tau^{(P)}} + j\left(\beta_s^{(P)} L_P + \beta_f^{(N)} L_N\right)\right) \\ & + \frac{1}{\Delta\tau^{(N)}} \kappa_{sf}^{(N)}\left(L_P + L_N + \frac{t}{\Delta\tau^{(N)}}\right) \exp\left[j\Delta\beta_{sf}^{(N)} \frac{t}{\Delta\tau^{(N)}} + j\left(\beta_s^{(P)} - \Delta\beta_{sf}^{(N)}\right) L_P + j\beta_f^{(N)} L_N\right] \end{aligned} \tag{11}$$

The non-zero temporal range of h_{sf} can be found to be $0 \le t \le \Delta\tau^{(P)} L_P$. Similarly, h_{fs} can be derived and its non-zero temporal range is $-\Delta\tau^{(P)} L_P \le t \le 0$. Therefore, the overall temporal range of interaction between S and F modes is $\left[-\Delta\tau^{(P)} L_P, \Delta\tau^{(P)} L_P\right]$. The CIRS thus equals to $2\Delta\tau^{(P)} L_P$.

2.3 Impulse Response of DMGD compensated link

A DMGD compensation link contains multiple spans and each span comprises multiple compensation pairs as shown in Fig. 1. Due to the weak coupling assumption, only first-order coupling needs to be account. Therefore, in any possible paths from mode S at the transmitter to mode F at the receiver should contain only one coupling event. Hence h_{sf} can be calculated as a sum of the interference from all the direct coupling paths from the S mode to the F mode, i.e., h_{sf} can be expressed as the summation of K components where K is the total number of compensation pairs:

$$h_{sf}(t) = \sum_{k=1}^{K} h_{sf}^{(k)}(t). \tag{12}$$

Each component represents interference from all possible coupling paths in one compensation pair. Except for the DMGD compensating pair where the coupling occurs, the signal stays in one mode when passing other pairs. Thus, zero MDG is accumulated on other pairs. Consequently, for the path with its coupling location in the kth pair, the path delay of the

#201102 - $15.00 USD Received 12 Nov 2013; revised 31 Dec 2013; accepted 27 Jan 2014; published 18 Feb 2014

coupling light via coupling location $z=(k-1)(L_P+L_N)+\Delta z \quad (k=1,2...K)$ is determined by the local position $\Delta z \ (0<\Delta z<L_P+L_N)$ inside that pair.

$$T_p(z)=\begin{cases}\Delta\tau^{(P)}\Delta z & 0<\Delta z<L_P \\ \Delta\tau^{(N)}(\Delta z-L_N-L_P) & L_P<\Delta z<L_P+L_N\end{cases} \tag{13}$$

Therefore, the CIRS of the DMGD compensated link is the same as a single compensation pair. If an oversampling rate 2 is assumed, the RTL for time domain equalization can be calculated as following

$$N_{taps}=4\Delta\tau^{(P)}L_P R_s \tag{14}$$

According to Eq. (14), the RTL depends on MGD of a section of P-type fiber rather than the MGD of the whole link. It indicates that by using small compensation step- size, the RTL could be very low even with weak random mode coupling. This is a main result of this paper.

3. Simulation

For simplicity, P-type and N-type FMFs which can guide two LP modes are designed and simulated. In P-type fiber, the faster LP_{01} mode is labeled as mode 1. the slower LP_{11} mode is labeled as mode 2. Trench assisted graded index profile is used as in [10]. By adjusting the power index α, DMGDs can be tuned to be 100 ps/km for P-type FMF and −100ps/km for N-type across the C-band. The index profile and the design parameters are shown in Fig. 4. The effective index differences between the two LP modes are 2.9×10^{-3} and the chromatic dispersion coefficients are 21 ps/nm/km for both types of fiber.

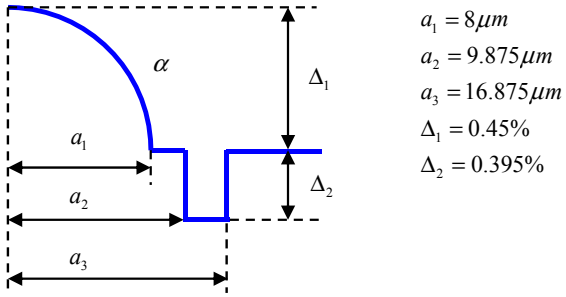

Fig. 4. Trench assisted graded index profile of P type ($\alpha = 2.079$) or N type ($\alpha = 2.196$).

Multi-section field propagation model was used to simulate two-mode transmission in FMF [9]. The section length was set to be 200m as same as [10]. For other section lengths such as 100m or 500m, negligible difference was observed. MSC was set to be −35dB/km which is slightly higher than the fiber with similar index profile used in [11] (−25dB crosstalk for 30km fiber, or −39.8dB/km). Losses were 0.2dB/km for both modes. No crosstalk was assumed from mode MUX/DEMUX or splicing.

The simulation setup is similar to [1]. In the transmitter, two independent 28 Gbaud QPSK signal streams were generated and multiplexed into two LP modes of FMF link comprising 10 spans with a span length of 128km. Each span was constructed by splicing multiple compensation fiber pairs. At the end of each span, an ideal multimode EDFA was used to compensate losses for both modes. At the receiver, signals in the two modes were detected after an ideal mode de-multiplexer and two coherent receivers. Chromatic dispersion was compensated using a static frequency-domain equalizer before adaptive equalization. Time-domain equalization (TDE) was used to equalize the signal and estimate the impulse responses of the link due to its freedom to have arbitrary tap lengths.

#201102 - $15.00 USD Received 12 Nov 2013; revised 31 Dec 2013; accepted 27 Jan 2014; published 18 Feb 2014

To verify the analytical solution, impulse responses were numerically analyzed for DMGD compensated and uncompensated links using the least mean square (LMS) method. Some typical impulse responses are shown in Fig. 5

For the DMGD uncompensated link, all 10 spans were constructed using the P-type fibers with a DMGD of 100ps/km. As shown in Fig. 5(a), impulse response h_{21} is confined in a center rectangular region. The width of region is 7162 taps which matches the estimated 7168-tap width by using Eq. (7). Figures 5(b)-5(c) shows h_{21} and h_{12} for the DMGD compensated link. The compensation step-size was set to be 64km which was half the span length. It is observed that the length of h_{21} and h_{12} is about 20 times shorter than that for the uncompensated link which agrees with theoretical analysis. Figure 5(d) illustrates the impulse response of h_{11}. The center peak corresponds to the signal from the uncoupled LP_{01} path. The pedestal, which is 30 dB down from the center peak of h_{11} and 15 dB down from the magnitudes of h_{21} and h_{12} is due to multipath interference which covers both the $t > 0$ and the $t < 0$ sides. In the model discussed in section 2, the multipath interference was ignored due to the weak coupling assumption. This simplification in the analytical model can introduce errors to the estimation of CIRS, particularly when MSC is high.

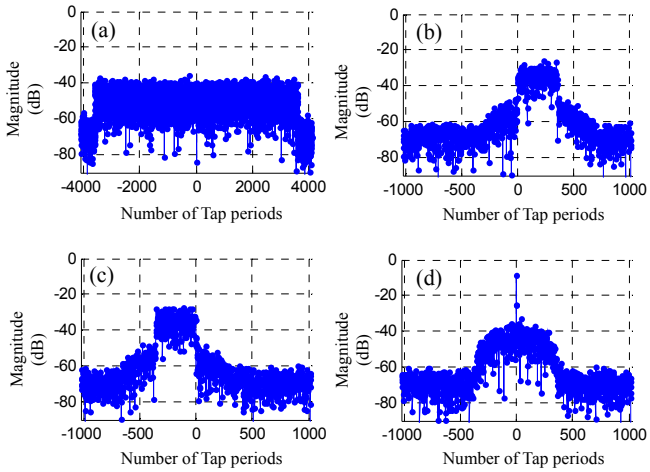

Fig. 5. Magnitude of impulse response Vs. number of tap periods for (a) h_{21} of 10 × 128km P-type fiber link; (b) h_{21}, (c) h_{12} and (d) h_{11} of 10 × (64km(P) + 64km(N)) DMGDC fiber link.

#201102 - $15.00 USD Received 12 Nov 2013; revised 31 Dec 2013; accepted 27 Jan 2014; published 18 Feb 2014

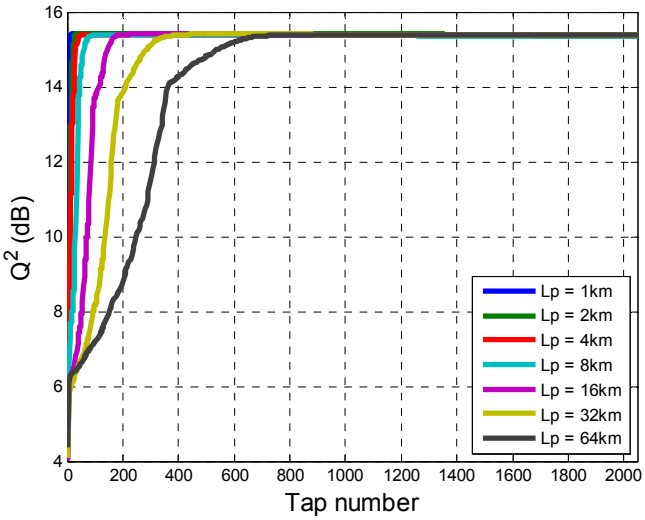

Fig. 6. Q^2 (dB) Vs. Tap number used in LMS equalizer when MSC = −35dB/km for 10 spans.

To rigorously analyze the RTL for the link, the receiving data are processed by equalizers with various tap lengths. The Q^2 factor as a function of tap length is plotted in Fig. 6. As the tap length increases, more distributed mode couplings or interferences are canceled leading to higher Q^2. When the tap length exceeds the CIRS, Q^2 converges to the maximum value determined by the OSNR at the receiver. Figure 6 also shows Q^2 curves for various compensation step size. For each curve, the RTL can be defined as the minimum tap length of the equalizer to achieve a 0.1dB Q^2 penalty compared to maximum achievable Q^2. Therefore, RTL as a function of compensation step-size can be plotted and is shown in Fig. 7 for different MSCs.

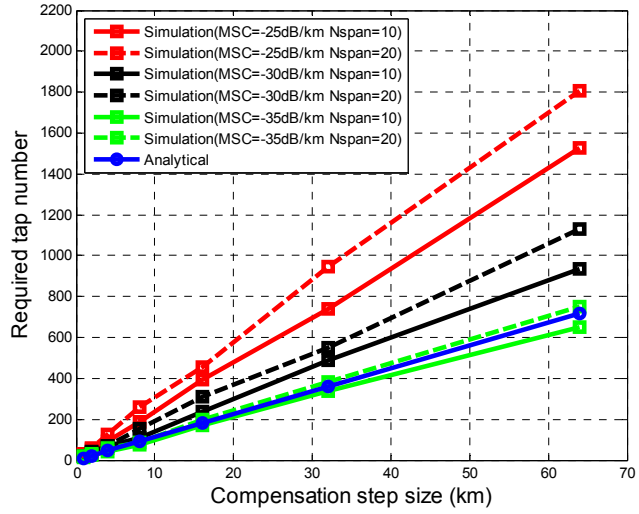

Fig. 7. Required tap number Vs. compensation step-size for various MSCs.

It is observed that for the case that MSC equals to −35dB/km, the numerical result agrees with analytical estimation well. According to Fig. 7, RTL can be reduced by decreasing compensation step-size. A similar conclusion is also reached in [3]. Here, we derived and further verified the linear scaling rule between RTL and the compensation step-size. When compensation step-size equals to 1km, the RTL is only 14 taps for 10 spans which is 1/512 of

#201102 - $15.00 USD Received 12 Nov 2013; revised 31 Dec 2013; accepted 27 Jan 2014; published 18 Feb 2014

that for uncompensated link when MSC equals to −35dB/km. As MSC increases, the analytical model underestimates RTL. Due to stronger random coupling, indirect coupling cannot be neglected any more. For MSC equals to −30dB/km or −25dB/km, the numerical result shows that the RTL is still linearly proportional to the compensation step size while slopes of the curves are larger when MSC is increased. Results for 20 spans are also plot in Fig. 7. Due to higher cumulated mode coupling, RTL for 20 spans link is larger than the one for 10 spans while the linear dependence on compensation step size still remains. It is worth to noting that by using ever smaller compensation step-sizes, CIRS of the entire link can be reduced to the level which is comparable to delay spread between degenerate modes. To achieve accurate estimation of CIRS in this regime, the degenerate mode dispersion must be taken account.

4. Conclusion

The equalizer tap length requirement has been investigated analytically and numerically for DMGD compensated links with weak random mode coupling. Unlike the DMGD uncompensated counterpart, the RTL of DMGD compensated link depends on the MGD of a single P-type or N-type fiber section. Although DMGD compensating fiber cannot reduce CIRS to zero when mode coupling has to be considered in practice, by using small compensation step-size, the RTL of DMGD-compensated links can be orders of magnitude shorter than that of DMGD uncompensated links.

Acknowledgement

This research was supported in part by the National Basic Research Programme of China (973) Project #2014CB340100.

#201102 - $15.00 USD Received 12 Nov 2013; revised 31 Dec 2013; accepted 27 Jan 2014; published 18 Feb 2014